THE JOURNAL OF BIOLOGICAL CHEMISTRY
Vol. 273, No. 18, Issue of May 1, pp. 11267–11273, 1998
Printed in U.S.A.

A Multifunctional Repeated Motif Is Present in Human Bifunctional tRNA Synthetase*

(Received for publication, December 2, 1997, and in revised form, February 2, 1998)

Seung Bae Rho‡, Jong Sang Lee‡, Eui-Jun Jeong§, Key-Sun Kim§, Yang Gyun Kim¶, and Sunghoon Kim‡‖

From the ‡Department of Biology, Sung Kyun Kwan University, 300 Chunchundong, Jangangu, Suwon, Kyunggido 440-746, Korea, the §Structural Biology Center, Korea Institute of Science and Technology, Cheongryang Box 131, Seoul 136-791, Korea, and the ¶Department of Biology, Massachusetts Institute of Technology, Cambridge, Massachusetts 02139

Tandem repeats located in the human bifunctional glutamyl-prolyl-tRNA synthetase (EPRS) have been found in many different eukaryotic tRNA synthetases and were previously shown to interact with another distinct repeated motifs in human isoleucyl-tRNA synthetase. Nuclear magnetic resonance and differential scanning calorimetry analyses of an isolated EPRS repeat showed that it consists of a helix-turn-helix with a melting temperature of 59 °C. Specific interaction of the EPRS repeats with those of isoleucyl-tRNA synthetase was confirmed by *in vitro* binding assays and shown to have a dissociation constant of approximately 2.9 μM. The EPRS repeats also showed the binding activity to the N-terminal motif of arginyl-tRNA synthetase as well as to various nucleic acids, including tRNA. Results of the present work suggest that the region comprising the repeated motifs of EPRS provides potential sites for interactions with various biological molecules and thus plays diverse roles in the cell.

Aminoacyl-tRNA synthetases are essential in protein synthesis, catalyzing the attachment of specific amino acids to cognate tRNAs. Despite the common catalytic role of these enzymes, cytoplasmic tRNA synthetases of higher eukaryotes differ from their lower eukaryotic or prokaryotic counterparts in forming a multiprotein complex (1–4). These multiprotein complexes are known to contain nine synthetases, which react with Glu, Pro, Ile, Leu, Met, Lys, Gln, Arg, and Asp (5). Although the presence of this complex in higher eukaryotic cells has been known for the last two decades, its functional significance and structural features remain elusive.

Among the tRNA synthetases of higher eukaryotes, glutamyl- and prolyl-tRNA synthetase activities have been found linked in a single polypeptide (6, 7). In human glutamyl-prolyl-tRNA synthetase (EPRS),[1] two domains exhibiting each enzyme activity are connected by a linker that contains three tandemly repeated motifs of 57 amino acids (7). The human prolyl-tRNA synthetase lacking this linker peptide was still active, suggesting that it is not essential for catalytic activity (8). This leaves the possibility that the linker region may play a distinct role in the cell other than the catalytic function.

Peptide sequences homologous to these repeats have also been found in other tRNA synthetases, although they are present as a single copy. They are located in the N-terminal extensions of glycyl- (9, 10), tryptophanyl- (11–13), and histidyl-tRNA synthetases (14, 15), which have been found as free forms, and in the C-terminal extension of methionyl-tRNA synthetase (16), which has been found in the complex. Although it is not clear whether they all play the same role in the cell, the prevalence of these motifs among the eukaryotic tRNA synthetases implies their functional significance.

EPRS of *Drosophila melanogaster* contains six tandem repeats of these motifs between the two catalytic domains. Overexpression of these motifs in transgenic flies resulted in a decrease of fertility (17). This result further supports the physiological importance of these motifs. It has been proposed that they may serve as a template for assembly of multisynthetase complex or as an anchor to link the complex to other cellular components, such as protein synthesis machinery (6, 17).

The three repeated motifs of human EPRS were previously shown to interact with the two repeated motifs present in the C-terminal extension of human cytoplasmic isoleucyl-tRNA synthetase (IRS) (18). The tandem repeats in human IRS are distinct from those of EPRS, and their homologues have not been found in other tRNA synthetases (19, 20). In the present work, we further analyzed the molecular interactions of the EPRS repeats with those of IRS and with other cellular molecules. Our results suggest that the peptide region containing the repeated motifs of EPRS is multifunctional and allows for multiple interactions with nucleic acids as well as with at least two different tRNA synthetases. Functional meaning of these interactions will be discussed.

EXPERIMENTAL PROCEDURES

Preparation of the EPRS Motif—DNA encoding one of the EPRS repeats (EPRS-R1) was isolated by polymerase chain reaction and subcloned into pET28a (Novagen) using *Eco*RI and *Xho*I. The motif was expressed in *Escherichia coli* strain BL21 (DE3) grown in M9 minimal medium supplemented with 0.3% glucose and 0.1% $^{15}NH_4Cl$. The His-tagged EPRS motif (from pHEPR1) (Table I) was purified using a Ni^{2+} column (Invitrogen), the His tag was cleaved off with thrombin, and the EPRS motif was further purified using C18 reverse phase high performance liquid chromatography (Waters 600). NMR samples containing approximately 2 mM isolated peptide in 90% H_2O/10% ^2H_2O were prepared by adjusting to pH 5.0 with NaO^2H. Samples for differential scanning calorimetry (DSC) were prepared by dialyzing the peptide overnight at 4 °C against 20 mM phosphate buffer (pH 5.0). DSC analysis was conducted at 1.0 mg/ml of the purified peptide. An extinction coefficient of 0.57 absorbance units/mg/ml was used to calculate the peptide concentration.

* This work was supported in part by Grant 94-0403-20 from the Korea Science and Engineering Foundation and by Hallym Grant 58-1801. The costs of publication of this article were defrayed in part by the payment of page charges. This article must therefore be hereby marked "*advertisement*" in accordance with 18 U.S.C. Section 1734 solely to indicate this fact.

‖ To whom correspondence should be addressed. Tel.: 82-331-290-7007; Fax: 82-331-290-7015; E-mail: shkim@yurim.skku.ac.kr.

[1] The abbreviations used are: EPRS, glutamyl-prolyl-tRNA synthetase; EPRS-R, EPRS repeat; IRS, isoleucyl-tRNA synthetase; IRS-R, IRS repeat; RRS, arginyl-tRNA synthetase; RRS-N, RRS N-terminal; DRS, aspartyl-tRNA synthetase; DRS-N, DRS N-terminal motif; DSC, differential scanning calorimetry; GST, glutathione *S*-transferase; BBD, biotin binding domain.

NMR Spectroscopy and DSC—The three-dimensional ^{1}H-^{15}N heteronuclear single quantum coherence-nuclear Overhauser enhancement spectroscopy and ^{1}H-^{15}N heteronuclear single quantum coherence-total correlation spectroscopy NMR spectra were recorded at 30 °C with a Varian UnityPlus 600-MHz spectrometer equipped with an actively shielded *z* gradient and a gradient amplifier unit (21). Assignments of cross-peaks were achieved in a sequential manner. The chemical shift index calculations and the estimation of secondary structure were carried out by the method of Wishart *et al.* (22). All chemical shifts used for the chemical shift index were from 2,2-dimethyl-2-silapentane-5-sulfonic acid. The DSC scan was carried out at the rate of 1 °C/min up to 100 °C using Nano-DSC (Calorimetry Science Corp.). To investigate the reversibility of protein folding, the second scan was performed at the same rate after cooling down to 25 °C.

In Vitro Binding Assay—DNA encoding the two repeats of IRS (Glu^{966}–Phe^{1266}) was ligated into pGEX4T-1 (Amersham Pharmacia Biotech) using *Eco*RI and *Sal*I to generate glutathione *S*-transferase (GST) fusion protein (pGIR12+) (Table I). DNA for the three repeats of EPRS (Asp^{677}–Thr^{884}) was ligated into pET28a. The human endothelial monocyte activating polypeptide II (EMAP II) (23) was also expressed as a His fusion protein and used as a control for binding assay. GST and His fusion proteins were purified according to the manufacturer's protocols. The purified GST-IRS (5 μg) was mixed either with His-EPRS (10 μg) or with His-EMAP II (10 μg) in binding buffer (20 mM Na_2HPO_4, pH 7.8, 500 mM NaCl) and incubated at 25 °C for 30 min. The mixtures were added to 20 μl of Ni^{2+} column matrix and incubated at 25 °C for 30 min. The slurry was pelleted by centrifugation and washed with 200 μl of washing buffer (20 mM Na_2HPO_4, pH 6.0, 500 mM NaCl) three times. The pellet of the gel matrix was resuspended in 20 μl elution buffer (20 mM Na_2HPO_4, pH 6.0, 500 mM NaCl containing 400 mM imidazole) and incubated at 25 °C for 20 min to elute the bound His fusion proteins. The eluted proteins were separated by gel electrophoresis, and the proteins were detected by Coomassie staining.

Determination of Binding Affinity—Binding constant between the EPRS and IRS repeats was determined by surface plasmon resonance using BIAcore system (Biacore). The EPRS peptide (Val^{573}–Lys^{889}) was fused to a biotin binding domain (BBD) using PinPoint Xa-1 vector (ProMega). *E. coli* cells expressing BBD-EPRS fusion protein (from pBEPR123+) (Table I) were grown in 2xYT medium containing 2 μM biotin to an OD_{600} of 0.5–0.8. Expression of the peptide was induced by the addition of 0.5 mM isopropyl-1-thio-β-D-galactopyranoside for 4 h. The induced cells were then harvested and resuspended in 20 mM Tris-HCl (pH 8.0) containing 10% glycerol, 50 mM NaCl, 0.1 mM EDTA, 1 mM dithiothreitol. Cells were lysed by ultrasonication, and the lysate was centrifuged to remove cell debris. The biotinylated fusion peptide was purified using SoftLink Soft Release Avidin Resin (ProMega). The fractions containing the peptide were pooled and dialyzed against 10 mM HEPES (pH 7.4), 10% glycerol, 50 mM NaCl, 0.1 mM EDTA, 1 mM dithiothreitol. The peptide was further purified by fast protein liquid chromatography using Mono-S ion exchange and gel filtration columns (Amersham Pharmacia Biotech).

BBD-EPRS was attached onto a streptavidin-coated sensor chip at 0.2 mg/ml to get about 1000 response units. The EPRS repeats without biotin binding domain did not bind to the chip under these conditions (500 mM NaCl), which suggests that BBD-EPRS was bound to the chip surface via the interaction between the fused BBD and streptavidin on the chip (data not shown). The chip was then washed with phosphate-buffered saline to remove the unbound BBD-EPRS. After recovering a flat base line, 25 μl of the purified GST-IRS solution at concentrations of 5 and 10 μM were passed over the EPRS-coupled chip at a flow rate of 10 μl/min for 2.5 min to record association between the two peptides. After 3 min, the bound IRS was dissociated by passing the buffer without IRS at the same flow rate. Parameters for association and dissociation of the two peptides were determined by BIAevaluation software based on the obtained sensogram.

Two Hybrid Analysis—Interactions of the EPRS repeats with unique peptide motifs found in other human tRNA synthetases were analyzed by the yeast two hybrid system (24). DNA fragment encoding the N-terminal motif (Met^{1}–Asn^{72}) of the human RRS was isolated by polymerase chain reaction using pM182 (kindly provided by Dr. K. Shiba, Cancer Institute, Tokyo, Japan). Oligonucleotide encoding the N-terminal motif (Thr^{5}–Glu^{26}) of human DRS was chemically synthesized. DNA fragments encoding one of the repeats (R3) in human EPRS (Glu^{828}–Thr^{884}) and one of the C-terminal repeats (R2) in IRS (Ser^{1169}-Phe^{1266}) were also obtained by polymerase chain reaction. All of these DNA fragments were introduced next to the genes for LexA and B42 to be expressed as fusion proteins. Each of the LexA and B42 fusion proteins were introduced into the testing yeast strain, EGY48, and the interaction between the fused synthetase motifs was determined by the ability to support cell growth on leucine-depleted medium (18).

Affinity Co-electrophoresis—Nucleic acid binding of the EPRS repeats was investigated by affinity co-electrophoresis following the method described previously (25). His fusion protein containing the EPRS repeats (Val^{573}–Lys^{889}) was generated (from pHEPR123+) (Table I). The expressed His-EPRS was purified by Ni^{2+} affinity and subsequently by Mono-S column chromatography (Amersham Pharmacia Biotech). Various DNA and RNA preparations labeled with ^{32}P were used for the binding assays. Total yeast tRNA mixture was purchased from Boehringer-Mannheim. $Minihelix^{Ala}$ (26) was obtained from the laboratory of Dr. Schimmel (Massachusetts Institute of Technology), and 50–60 base pair calf thymus DNA was prepared by sonication and gel electrophoresis. Nucleic acid preparations were labeled with ^{32}P using polynucleotide kinase after removing 5′ phosphate with calf intestine phosphatase. The purified His-EPRS at various concentrations (0.004–3.6 μM) was mixed with 5% polyacrylamide solution. After preparation of the gel, the radioactively labeled nucleic acids were loaded into the vertically oriented well. After electrophoresis, the radioactive nucleic acids and their complexes were visualized by autoradiography.

Dissociation constants (K_D) of the EPRS repeats and various nucleic acids were determined as described previously (27). The mobility shifts of the EPRS-nucleic acid complexes were measured and divided by the maximal possible shift to obtain the values of relative shift (*R*). The *R* values were subsequently divided by the respective concentrations of EPRS used for each lane. Scatchard plots of *R versus R*/[EPRS] give linear lines, the slopes of which are equivalent to $-1/K_D$. The dissociation constants for tRNA, minihelix, and carrier DNA were determined from values obtained three, two, and one independent experiments, respectively.

RESULTS

Structure and Conformational Stability of the EPRS Motif—Human EPRS contains three repeated units consisting of 57 amino acids (Fig. 1*A*). Secondary structure predictions of the motif suggested that it would form an α-helix (6, 17, 18). To determine the structure and stability in folded configuration, one of the repeated motifs (EPRS-R1) was subjected to NMR and DSC analyses. The chemical shift index of HCα in this motif indicates that the EPRS motif consists of two helices (residues 1–23 and 26–43) and a possible C-terminal β-sheet (residues 48–50) (Fig. 1*B*). The secondary structure profile of the NMR analysis is consistent with the computer prediction and suggests that it may form a helix-turn-helix or a dimer with intermolecular helix-helix interactions. However, the ratio of van't Hoff to calorimetric enthalpy (28), which is close to 1, supports a helix-turn-helix fold rather than a dimeric fold. The DSC thermogram indicates that the EPRS motif unfolds at 59 °C and has an enthalpy of 51 kcal/mol, which further supports the compactness of the structure (Fig. 1*C*). The folding of this protein was completely reversible, with enthalpy recovery of higher than 95% for the second DSC scan.

In Vitro Interaction and Binding Affinity between the EPRS and IRS Repeats—Interaction between the repeated motifs of EPRS and IRS was previously shown by genetic analysis (18). The interaction was further tested by an affinity co-purification experiment. The His-EPRS fusion protein was mixed with GST-IRS, and the mixture was purified employing Ni^{2+} column matrix. GST-IRS was co-purified with His-EPRS but not with His-EMAP II as a bound complex (Fig. 2). Similar results were obtained when the mixtures were purified by affinity of GST-IRS to glutathione column matrix (data not shown). These results confirmed the specific interaction between the repeats of EPRS and IRS.

We then determined the binding affinity between the EPRS and IRS repeated motifs by surface plasmon resonance using BIAcore system. Nonspecific binding of the isolated EPRS to the sensor chip was observed at 150 mM NaCl but not at 500 mM NaCl (data not shown). To avoid nonspecific binding of

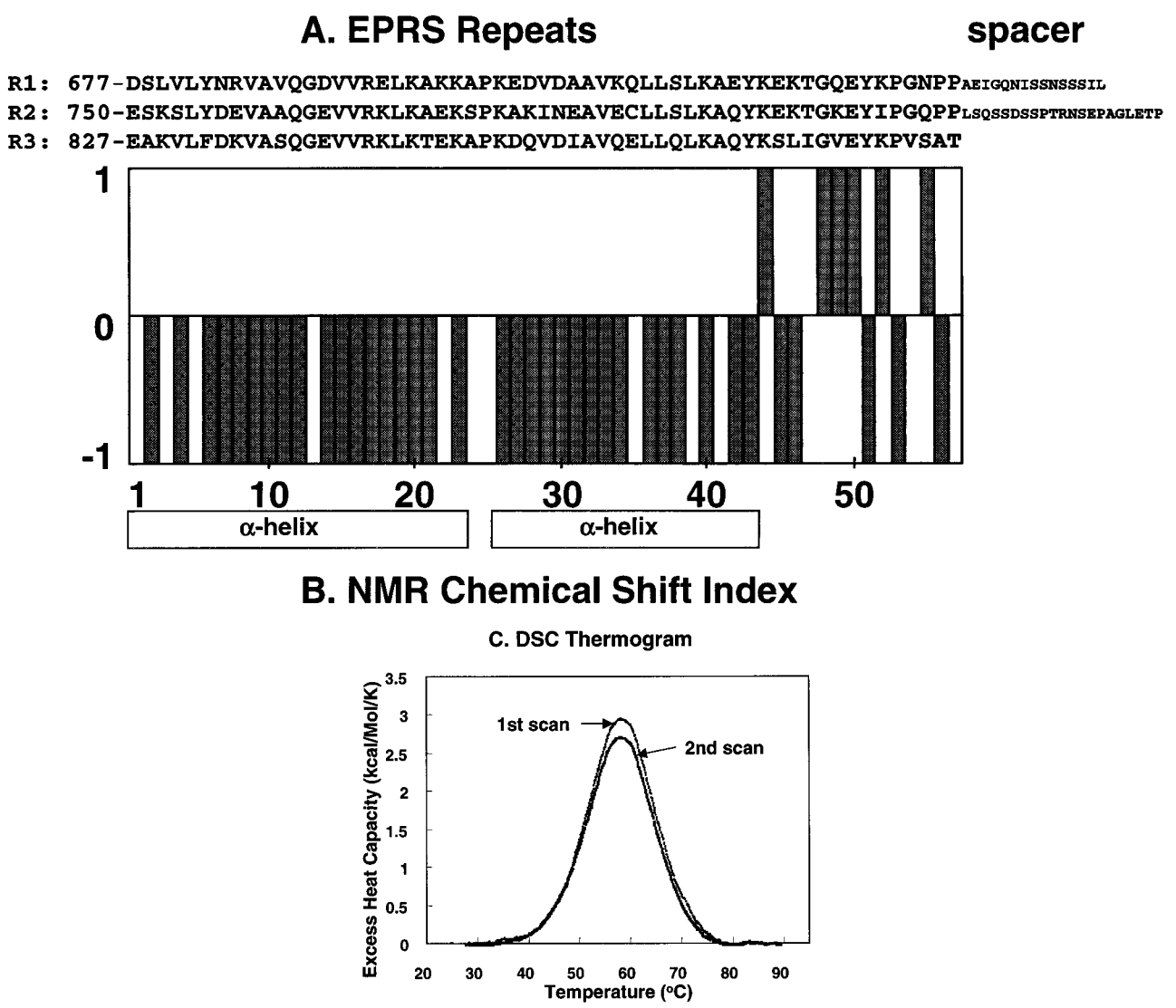

FIG. 1. **Sequence, structure, and folding of the repeated motif of EPRS.** *A*, three repeats of human EPRS (R1-R3) and spacer sequences are shown. *B*, the isolated EPRS-R1 was subjected to NMR analysis. The chemical shift index calculation and the estimation of secondary structure were generated according to the method of Wishart *et al.* (22). Briefly, chemical shifts of HCα were compared with random coil values. The values +1 and −1 indicate greater and less than random coil values, respectively. Grouping of −1 and +1 predicts α-helix and β-sheet, respectively. *Boxes* indicate the predicted α-helical regions. *C*, temperature dependence of the excessive heat capacity of EPRS-R1. Integration under the curve gives an enthalpy at transition temperature. The first scan was monitored at the rate of 1 °C/min up to 100 °C, and the determined T_m was 59 °C. The second scan was carried out after cooling down the solution containing the peptide to 25 °C.

EPRS onto the sensor chip and to better orient the peptide for the binding study, we fused the EPRS repeats to a biotin binding domain (pBEPR123+) (Table I) and attached the biotinylated EPRS onto a streptavidin-coated chip at 500 mM NaCl. Subsequently, the purified GST-IRS (from pGIR12+) (Table I) was passed over the EPRS-coupled streptavidin chip, and the binding was monitored (Fig. 3). Association of the two proteins was monitored by the increase in response unit. Nonspecific binding of GST-IRS fusion protein to the streptavidin chip was not observed under the experimental conditions employed (data not shown). The buffer without IRS was then added to the chip to monitor dissociation of the two proteins. Average association (k_{on}) and dissociation (k_{off}) rate constants measured from the response of sensogram were $1.25 \pm 0.42 \times 10^3$ $M^{-1}s^{-1}$ and $3.08 \pm 0.29 \times 10^{-3}s^{-1}$, respectively. From these values, the dissociation constant between the two molecules was estimated to be 2.9 ± 1.2 μM.

Interaction of the EPRS Repeats with the N-terminal Motif in RRS—Human DRS and RRS contain unique N-terminal extensions. These peptides in mammalian enzymes have been shown

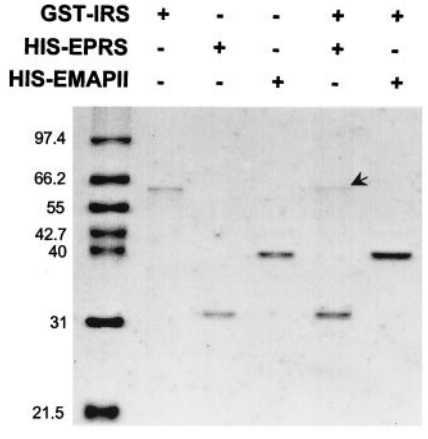

FIG. 2. **Co-purification of EPRS and IRS.** The His-EPRS (30 kDa) and His-EMAP II (41 kDa) fusion proteins were mixed with GST-IRS (62 kDa). The mixtures were subjected to Ni^{2+} affinity purification. Co-purification of GST-IRS with His-EPRS, but not with His-EMAP II, is shown by the *arrow*.

TABLE I

Fusion proteins of human aminoacyl-tRNA synthetase motifs used for experiments

Peptide regions of four human tRNA synthetases (AARS) were fused to His, GST, and BBD for structural and *in vitro* binding analyses. They were also fused to LexA (DNA binding domain) and B42 (transcription activation domain) for yeast two hybrid assay. R stands for the repeated motifs of EPRS and IRS, and N stands for the N-terminal motifs of RRS and DRS.

Plasmid	Tag	AARS	Motif	No. of amino acids
pHEPR123+	His_6	EPRS	R123+ (Val^{573}–Lys^{889})	317
pHEPR123	His_6	EPRS	R123 (Asp^{677}–Thr^{884})	208
pBEPR123+	BBD	EPRS	R123+ (Val^{573}–Lys^{889})	317
pHEPR1	His_6	EPRS	R1 (Asp^{677}–Pro^{733})	57
pLEPR123+	LexA	EPRS	R123+ (Val^{573}–Lys^{889})	317
pLEPR123	LexA	EPRS	R123 (Asp^{677}–Thr^{884})	208
pLEPR12	LexA	EPRS	R12 (Asp^{677}–Pro^{806})	130
pLEPR23	LexA	EPRS	R23 (Glu^{750}–Thr^{884})	135
pLEPR1	LexA	EPRS	R1 (Asp^{677}–Pro^{733})	57
pLEPR2	LexA	EPRS	R2 (Glu^{750}–Pro^{806})	57
pLEPR3	LexA	EPRS	R3 (Glu^{828}–Thr^{884})	57
pBEPR3	B42	EPRS	R3 (Glu^{828}–Thr^{884})	57
pGIR12+	GST	IRS	R12+ (Glu^{966}–Phe^{1266})	301
pLIR2	LexA	IRS	R2 (Ser^{1169}–Phe^{1266})	98
pBIR2	B42	IRS	R2 (Ser^{1169}–Phe^{1266})	98
pLRN	LexA	RRS	N (Met^{1}–Asn^{72})	72
pBRN	B42	RRS	N (Met^{1}–Asn^{72})	72
pLDN	LexA	DRS	N (Thr^{5}–Glu^{26})	22
pBDN	B42	DRS	N (Thr^{5}–Glu^{26})	22

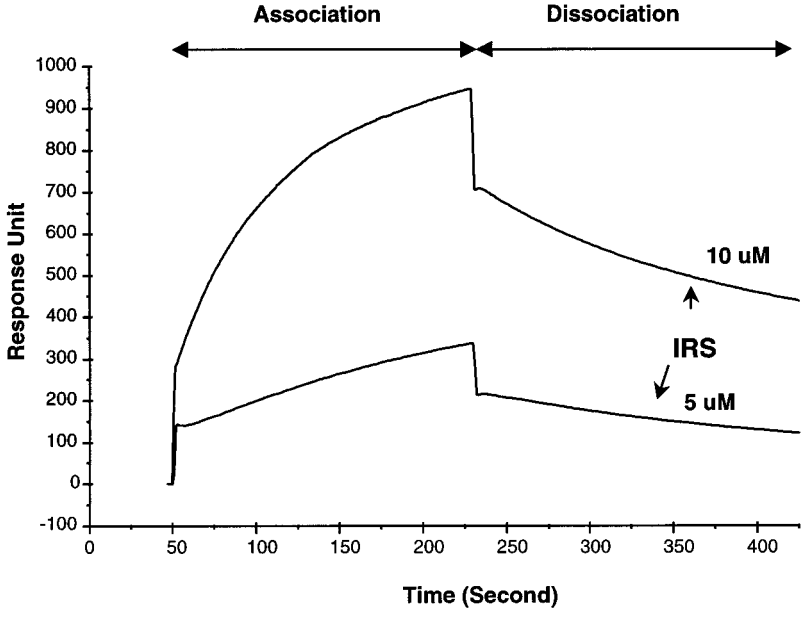

FIG. 3. **Determination of binding affinity between peptides containing EPRS and IRS motifs.** Binding affinity between the peptides containing the EPRS and IRS motifs was determined using BIAcore. The biotinylated EPRS peptide was coupled to a streptavidin-coated sensor chip. Buffers containing GST-IRS fusion protein (5 and 10 μM) were poured over this chip to measure association between the two peptides. Subsequently, buffer alone was flowed over the chip to measure dissociation of the peptides. The dissociation constant was determined by BIAevaluation software.

to be responsible for the formation of multisynthetase complex (29–31). The N-terminal motifs of human DRS (32, 33) and RRS (34, 35) are predicted to form α-helices (Fig. 4*A*). Because EPRS is a component of the multisynthetase complex, it is possible that the repeated motifs of EPRS are involved in multivalent protein-protein interactions with other synthetases. We tested the possibility as to whether the N-terminal extensions of DRS and RRS interact with the EPRS repeats using the yeast two hybrid method.

The motifs present in the four tRNA synthetases were fused to the DNA binding domain, LexA, as well as to the transcriptional activator, B42 (Fig. 4*A*; Table I). Interactions between all of the sixteen combinations between the four unique motifs of EPRS-R3, IRS-R2, DRS-N, and RRS-N were tested. Among the tested combinations, only the pair between the EPRS and IRS motifs showed positive interaction (Fig. 4*B*). Subsequently, interactions of the DRS and RRS motifs with the EPRS protein were further studied using the peptides containing different numbers of the repeated motifs (pLEPR series) (Table I). The N-terminal motif of RRS showed an interaction with the EPRS containing three repeats but did not bind to those containing fewer than three (Fig. 4*C*). In contrast, the N-terminal motif of DRS did not show an interaction with any of the EPRS motifs tested. These results suggest that the three repeats of EPRS make additional interactions with the N-terminal motif of RRS.

Nucleic Acid Binding of the EPRS Repeats—Most eukaryotic tRNA synthetases show an affinity to polyanions, such as nucleic acids (36, 37) and heparin (38). The repeated motifs of EPRS contain a high proportion of positively charged amino acids (about 20%), especially in the central region of the repeated motifs. Therefore, we expected that the EPRS motifs may be able to bind to nucleic acids. Interaction of the EPRS motifs with various nucleic acids was investigated by affinity co-electrophoresis. ^{32}P-labeled yeast total tRNA, minihelix^{Ala}, and calf thymus DNA of 50–60 base pairs were used for the binding assays. His-EPRS (from pHEPR123+) (Table I) was mixed with the radioactively labeled nucleic acids and subjected to electrophoresis. His-EPRS formed complexes with all of the tested nucleic acids (Fig. 5). The observed apparent dissociation constants were approximately 0.016 μM for yeast tRNA, 0.031 μM for minihelix, and 0.027 μM for calf thymus

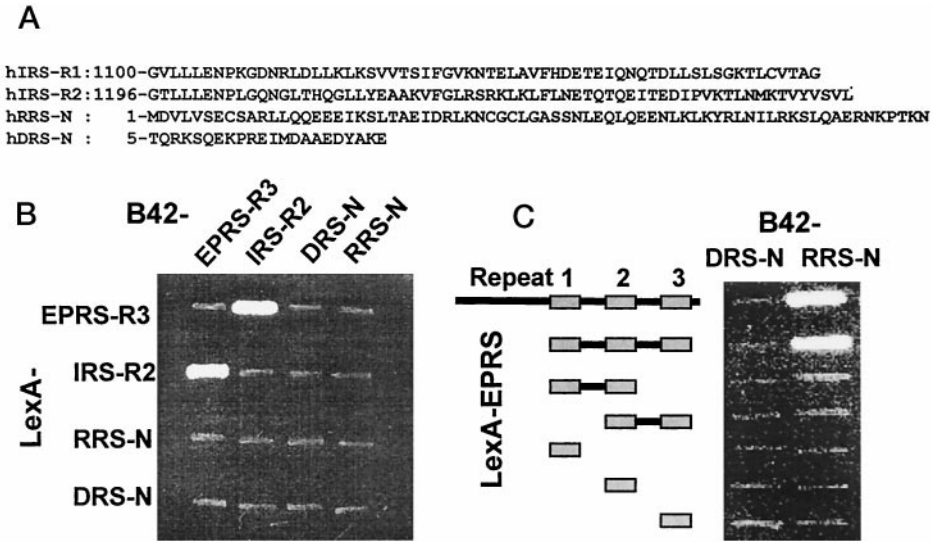

FIG. 4. **Interaction of EPRS repeated motifs with N-terminal extension of RRS.** *A*, peptides containing the unique motifs of EPRS-R3 (Fig. 1*A*), IRS-R2, DRS-N, and RRS-N were fused to LexA (DNA binding domain) and B42 (transcriptional activator) for the determination of interaction using yeast two hybrid system (24). *B*, self and heterologous interactions between the four motifs were analyzed in a reciprocal manner. Positive interactions between the two peptides were determined by yeast cell growth on leucine-depleted media. *C*, peptides containing different numbers of the EPRS motifs were fused to LexA, and their interactions with the N-terminal motifs of DRS and RRS were determined by the cell growth on leucine-depleted medium.

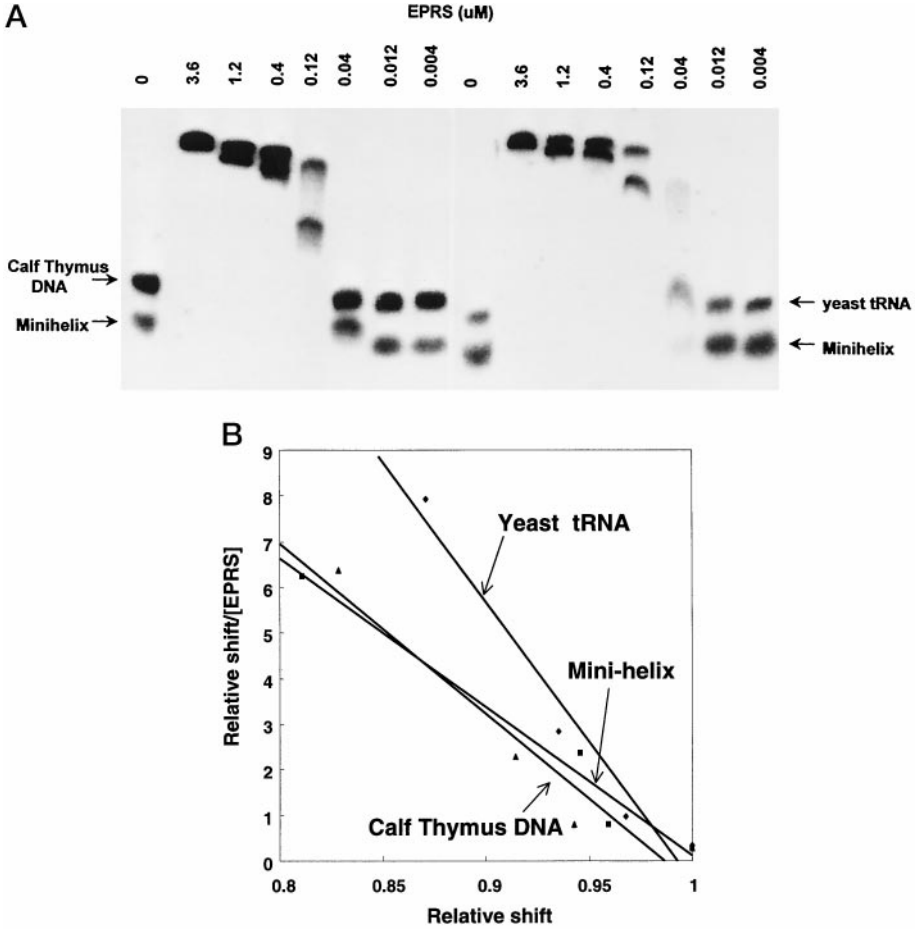

FIG. 5. **Nucleic acid binding activity of EPRS repeats determined by affinity co-electrophoresis.** *A*, His-EPRS (from pHEPR123+) (Table I) was mixed with 5% polyacrylamide solution at the indicated concentrations. Pairs of radioactively labeled nucleic acids were then subjected to electrophoresis in the peptide containing gel matrix to monitor the binding of the peptide to nucleic acids. *B*, Scatchard plots of the EPRS binding to various nucleic acids to determine dissociation constants (K_D). The plots of relative shift (R) *versus* R/[EPRS] (μM^{-1}) for each nucleic acid were made. The slope is equivalent to $-1/K_D$ (27).

DNA when estimations were done following the previously described procedure (27). These results suggest that the EPRS repeats poorly distinguish different nucleic acids, although they showed a slight preference for tRNA over calf thymus DNA and minihelix. However, the EPRS repeats did not bind to single stranded poly$(dA)_{30}$ (data not shown), suggesting that they may recognize helical backbone of double stranded nucleic acids.

DISCUSSION

The physiological significance of the association between the different eukaryotic tRNA synthetases has been a long-stand-

ing question. The structure and function of the multisynthetase complex are thought to be related to the newly evolved unique peptides present in the tRNA synthetases of higher eukaryotes (3, 4). To get an insight into the functions of these peptides, we focused on the repeated motifs of EPRS located between the two catalytic domains and investigated their structure and interactions. The results of NMR and DSC suggested that these repeats form a stably folded helix-turn-helix (Fig. 1, *B* and *C*). The well defined structure of these repeats suggests that they may not be a simple linker of the two catalytic domains. The marginal and spacer regions of the repeated motifs in EPRS contain a high proportion of proline and small amino acids, such as glycine, alanine, and serine. The peptides rich in these residues may form flexible turns between the repeated motifs (Fig. 1*A*). Thus, the repeated motifs of EPRS may form a higher order conformation rather than a linear structure. The complex three-dimensional structure of these repeats may be responsible for the multiple interactions with various molecules, as shown in this work.

The structure and function of the unique peptides in the eukaryotic tRNA synthetases have been extensively studied in the case of the N-terminal extension of eukaryotic DRS, which is one of the components of the complex. The N-terminal truncated DRS did not associate to the multisynthetase complex in the cell (29), suggesting a role of the N-terminal extension as a complex association domain. However, this domain, when fused to a heterologous protein, did not drive the protein to the complex. It is thus implied that additional interactions via the connected catalytic domain are required to determine the complex formation of DRS. The N-terminal extension of DRS was also shown to bind to tRNA and elongation factor, thereby facilitating the transfer of the bound aspartyl-tRNA for protein synthesis (39, 40). These results suggest that the N-terminal extension of DRS plays versatile roles in the cell as a domain responsible for association to tRNA synthetases and other molecules and also as a channel for tRNA delivery.

The known functions of the DRS extension can be extrapolated to the case of the EPRS repeats. We demonstrated in the present work that the EPRS repeats are involved in specific interaction with IRS (Figs. 2 and 4). The determined dissociation constant between the EPRS and IRS repeats (Fig. 3) is about 100-fold higher than that between DRS and the multisynthetase complex (30). Assuming that all of the components are bound to the complex with a similar binding stability, the interaction between the repeats of EPRS and IRS may not be strong enough to keep the two proteins within the complex. Thus, assembly of the two enzymes to the native complex should be aided by additional interactions. The association of these proteins to the complex can be further contributed to by the interactions with other molecules attracted to the repeated motifs as well as by the interactions of the catalytic domains of EPRS and IRS. In this work, we showed that the EPRS repeats also bind to the N-terminal extension of RRS (Fig. 4*C*). The interaction between the repeats of EPRS with IRS may be stabilized by their additional interaction with RRS.

The nucleic acid binding activity of the EPRS repeats (Fig. 5) can function as a channel of tRNA for catalysis and protein synthesis, stabilizer of protein-protein interaction, and cellular localization signal of the synthetase complex. Yeast Arc1p protein bound to cytoplasmic methionyl-tRNA synthetase and glutamyl-tRNA synthetase showed the binding activity to tRNA (41). The proposed role of this protein was to facilitate the binding and delivery of tRNA to the catalytic site of the bound tRNA synthetases. Perhaps the EPRS repeats were a functional homologue of yeast Arc1p and later genetically fused to a catalytic domain of various tRNA synthetases during evolution.

Although the EPRS repeats were not essential for the activity of the connected tRNA synthetase (8), overexpression of these repeats in *Drosophila* resulted in sterility (17). Similarly, a mutation of the gene for yeast Arc1p induced slow growth and cold sensitivity of the cell, although it was not essential for the activities of the bound tRNA synthetases (41). These results together imply that the *in vivo* function of the EPRS repeats could be more significant and pleiotropic than what they appear to be from the experimental results of isolated *in vitro* systems.

The results of the present study indicate that there is much similarity between the EPRS repeats and the N-terminal extension of DRS in their structure and interactions. Many other eukaryotic tRNA synthetases also contain unique peptides of similar structural and functional features. All of these peptides are thus expected to play versatile roles in the cell in a similar fashion. The functional versatility would result from the potential of these peptides to accommodate multiple interactions with diverse cellular molecules.

Most of the conserved residues among the EPRS repeats are hydrophobic and positively charged (6). Because interactions between eukaryotic tRNA synthetases have been reported to be driven by hydrophobic interactions (2, 29), these protein-protein interactions are expected to be mediated by hydrophobic residues of the repeated motifs. In contrast, interactions with nucleic acids are likely to involve charged residues. Thus, the repeated motifs of EPRS may be simultaneously involved in protein-protein and protein-nucleic acid interactions using different residues in the motifs. In summary, all of the proposed roles of the unique eukaryotic peptides, including the EPRS repeats, may not be mutually exclusive and can be sequentially or simultaneously achieved in the cell via their versatility of interaction. The complex formation of the tRNA synthetases could provide a means for these peptides to work together in a concerted manner.

Acknowledgments—We thank Drs. K. Manoharan, K. Shiba, S. Martinis, and K. Musier-Forsyth for critical reading and comments and C. Lee and S. G. Park for materials.

REFERENCES

1. Dang, C. V., and Dang, C. V. (1986) *Biochem. J.* **239,** 249–255
2. Deutscher, M. P. (1984) *J. Cell Biol.* **99,** 373–377
3. Mirande, M. (1991) *Prog. Nucleic Acid Res. Mol. Biol.* **40,** 95–142
4. Kisselev, L. L., and Wolfson, A. D. (1994) *Prog. Nucleic Acid Res. Mol. Biol.* **48,** 83–142
5. Mirande, M., Le Corre, D., and Waller, J.-P. (1985) *Eur. J. Biochem.* **147,** 281–289
6. Cerini, C., Kerjan, P., Astier, M., Gratecos, D., Mirande, M., and Semeriva, M. (1991) *EMBO J.* **10,** 4267–4277
7. Fett, R., and Knippers, R. (1991) *J. Biol. Chem.* **266,** 1448–1455
8. Heacock, D., Forsyth, C. J., Shiba, K., and Musier-Forsyth, K. (1996) *Bioorg. Chem.* **24,** 273–289
9. Nada, S., Chang, P. K., and Dignam, J. D. (1993) *J. Biol. Chem.* **268,** 7660–7667
10. Shiba, K., Schimmel, P., Motegi, H., and Noda, T. (1994) *J. Biol. Chem.* **269,** 30049–30055
11. Frolova, L. Y., Sudomoina, M. A., Grigorieva, A. Y., Zinovieva, O. L., and Kisselev, L. L. (1991) *Gene* **109,** 291–296
12. Garret, M., Pajot, B., Trezeguet, V., Labouesse, J., Merle, M., Gandar, J. C., Benedetto, J. P., Sallafranque, M. L., Alterio, J., Gueguen, M., Sarger, C., Labouesse, B., and Bonnet, J. (1991) *Biochemistry* **30,** 7809–7817
13. Lee, C. C., Craigen, W. J., Muzny, D. M., Harlow, E., and Caskey, C. T. (1990) *Proc. Natl. Acad. Sci. U. S. A.* **87,** 3508–3512
14. Tsui, F. W., and Siminovitch, L. (1987) *Nucleic Acids Res.* **15,** 3349–3367
15. Tsui, F. W., and Siminovitch, L. (1987) *Gene* **61,** 349–361
16. Lage, H., and Dietel, M. (1996) *Gene* **178,** 187–189
17. Cerini, C., Semeriva, M., and Gratecos, D. (1997) *Eur. J. Biochem.* **244,** 176–185
18. Rho, S. B., Lee, K. H., Kim, J. W., Shiba, K., Jo, Y. J., and Kim, S. (1996) *Proc. Natl. Acad. Sci. U. S. A.* **93,** 10128–10133
19. Nichols, R. C., Raben, N., Boerkoel, C., and Plotz, P. H. (1995) *Gene* **155,** 299–304
20. Shiba, K., Suzuki, N., Shigesada, K., Namba, Y., Schimmel, P., and Noda, T. (1994) *Proc. Natl. Acad. Sci. U. S. A.* **91,** 7435–7439
21. Zhang, O., Kay, L. E., Olivier, J. P., and Forman-Kay, J. D. (1994) *J. Biomol.*

NMR **4,** 845–858
22. Wishart, D. S., Sykes, B. D., and Richards, F. M. (1992) *Biochemistry* **31,** 1647–1651
23. Kao, J., Houck, K., Fan, Y., Haehnel, I., Libutti, S. K., Kayton, M. L., Grikscheit, T., Chabot, J., Nowygrod, R., Greenberg, S., Kuang, W.-J., Leung, D. W., Hayward, J. R., Kisiel, W., Heath, M., Brett, J., and Stern, D. M. (1994) *J. Biol. Chem.* **269,** 25106–25119
24. Gyuris, J., Golemis, E., Chertkov, H., and Brent, R. (1993) *Cell* **75,** 791–803
25. Cilley, C. D., and Williamson, J. R. (1997) *RNA* **3,** 57–67
26. Hou, Y.-M., Francklyn, C., and Schimmel, P. (1989) *Trends Biochem. Sci.* **14,** 233–237
27. Lim, W. A., Sauer, R. T., and Lander, A. D. (1991) *Methods Enzymol.* **208,** 196–210
28. Privalov, P. L., and Potekhin, S. A. (1986) *Methods Enzymol.* **131,** 4–15
29. Mirande, M., Lazard, M., Martinez, R., and Latreille, M. T. (1992) *Eur. J. Biochem.* **203,** 459–466
30. Agou, F., and Mirande, M. (1997) *Eur. J. Biochem.* **243,** 259–267
31. Lazard, M., and Mirande, M. (1993) *Gene* **132,** 237–245
32. Jacobo-Molina, A., Peterson, R., and Yang, D. C. H. (1989) *J. Biol. Chem.* **264,** 16608–16612
33. Escalante, C., and Yang, D. C. H. (1993) *J. Biol. Chem.* **268,** 6014–6023
34. Girjes, A. A., Hobson, K., Philip, C., and Lavin, M. F. (1995) *Gene* **164,** 347–350
35. Vellekamp, G., Sihag, R. K., and Deutscher, M. P. (1985) *J. Biol. Chem.* **260,** 9843–9847
36. Alzhanova, A. T., Fedorov, A. N., Ovchinnikov, L. P., and Spirin, A. S. (1980) *FEBS Lett.* **120,** 225–229
37. Alzhanova, A. T., Fedorov, A. N., and Ovchinnikov, L. P. (1982) *FEBS Lett.* **144,** 149–153
38. Cirakoglu, B., and Waller, J.-P. (1985) *Eur. J. Biochem.* **151,** 101–110
39. Reed, V. S., and Yang, D. C. H. (1994) *J. Biol. Chem.* **269,** 32937–32941
40. Reed, V. S., Wasteny, M. E., and Yang, D. C. H. (1994) *J. Biol. Chem.* **269,** 32932–32936
41. Simos, G., Segref, A., Fasiolo, F., Hellmuth, K., Shevchenko, A., Mann, M., and Hurt, E. C. (1996) *EMBO J.* **15,** 5437–5448